THE AMERICAN SOCIETY OF MECHANICAL ENGINEERS
345 E. 47th St., New York, N.Y. 10017

97-GT-362

Three-Dimensional Computation of Gas Turbine Combustors And The Validation Studies of Turbulence And Combustion Models

D. Biswas, K. Kawano, H. Iwasaki and M. Ishizuka
Research and Development Center,
Toshiba Corporation,
Kawasaki, Japan
and
S. Yamanaka
Heavy Apparatus Engineering Laboratory,
Toshiba Corporation,
Yokohama, Japan

ABSTRACT

The main aim of the present work is to explore computational fluid dynamics and related turbulence and combustion models for application to the design, understanding and development of gas turbine combustor. Validation studies were conducted using the Semi-Implicit Method for Pressure Linked Equations (SIMPLE) scheme to solve the relevant steady, elliptical partial differential equations of the conservation of mass, momentum, energy and chemical species in three-dimensional cylindrical co-ordinate system to simulate the gas turbine combustion chamber configurations. A modified version of k-ε turbulence model was used for characterization of local turbulence in gas turbine combustor. Since, in the present study both diffusion and pre-mixed combustion were considered, in addition to familiar bi-molecular Arhenius relation, influence of turbulence on reaction rates was accounted for based on the eddy break up concept of Spalding and was assumed that the local reaction rate was proportional to the rate of dissipation of turbulent eddies. Firstly, the validity of the present approach with the turbulence and reaction models considered is checked by comparing the computed results with the standard experimental data on recirculation zone, mean axial velocity and temperature profiles, etc. for confined, reacting and non-reacting flows with reasonably well defined boundary conditions. Finally, the results of computation for practical gas turbine combustor using combined diffusion and pre-mixed combustion for different combustion conditions are discussed.

NOMENCLATURE

A_1, A_2 : constants of combustion model
c_μ, $c_{\varepsilon 1}$, $c_{\varepsilon 2}$, c_1, c_2 : turbulence model constants
d : diameter
h : stagnation enthalpy
k : turbulence kinetic energy
m : mass fraction
p : pressure
R : stoichiometric ratio
R_j : reaction rate source term in the model equation
Ri : Richardson number
r : coordinate direction radius
T : temperature
u, v, w : velocity component in x, r and θ -direction
δ_{ij} : Kronecker delta
ε : dissipation rate of turbulence
μ : viscosity
ρ : density
σ : Prandtl/Scmidt number
ψ : stream function
ϕ_1, ϕ_2 : functions in turbulence model

Subscript
eff : Effective
i : Inner
O : Outer
fu : Fuel
ox : Oxidant
pr : Product
t : Turbulent

1. INTRODUCTION

Full predictions of the combustor flow field are desirable for a variety of valid reasons: a) to improve durability where some practical boundary conditions can be specified for the design and calculation of the liner cooling (Sturgess (1980)) b) to have some understanding of combustor behavior as a diagnostic tool during engine development programs c) to simulate scale-up and perturbations from base-condition effects during design and development (Novick, et al.

Presented at the International Gas Turbine & Aeroengine Congress & Exhibition
Orlando, Florida — June 2–5, 1997

(1979)) and d) to give assistance in planning and interpreting experimental programs. Therefore, a combustor flow field solver with sufficient accuracy, which can be used in the design process, is very much needed to combating the ever-increasing costs of rig programs and long lead times associated with experimental hardware. In developing such computational tool for the gas turbine combustor design, it is essential to thoroughly validate the performance of the individual physics-based models, assess the influence of the flow solver on solution accuracy, and establish that the overall procedures are workable in complex flows where all the separate effects must be treated simultaneously.

Several reports on computation of combustor flow are available in the literature, namely, Sturgess and Syed (1985), Vanka (1985), Kanniche and Zurbach (1995). In this combustor flow calculation, the time averaged Navier-Stokes equations, the species and energy equations are solved along with the k-ε turbulence model for closure coupled with a chemical equilibrium hypothesis.

The accurate prediction of combusting flows requires proper physics-based modeling of turbulence and combustion. Turbulence is the most complicated kind of fluid motion. Considerable progress has been made in understanding and describing the turbulence phenomena. A reasonably complete and up to date information is available in the report of Speziale (1991). Models of varying degrees of sophistication are available and depending on the complexity of the model the required computational time increases. A widely used approach to predict the turbulence characteristics is to use k-ε turbulence model for closure. However, the standard k-ε model need to be improved to adequately predict the complex swirling flow in the gas turbine combustor. In the present work a standard two-equations k-ε turbulence model is modified to take into account the secondary straining effect of swirl by formally operating on the algebraic Reynolds stress model. Since in the gas turbine combustor mixing of fuel and oxidant is achieved by introducing the oxidant into the combustor after a swirl motion being added. This approach, originally proposed by Kim-Chung(1987), is considerably cost-effective compared with the Reynolds stress model, due to the computational simplicity of the k-ε model.

Models of varying degrees of complexity are available for the time-averaged reaction rate of a chemical species in turbulent flow. In the flamelet models, the reaction zone is viewed as a collection of laminar flame elements controlled by turbulent flow. The reaction process is modeled under the chemical equilibrium hypothesis. Some of the recent models are made considerably complicated and computationally expansive by increasing the number of transport equations for scalar to be solved in modeling simultaneously the two types of combustion (diffusion and premix) in industrial combustors. Where the fuel may not burn completely and a diffusion flame may be formed between the fresh air and the excess fuel or between the excess air in lean zones and the excess fuel in reach zones, when the temperature of burned gases is sufficiently high to allow the ignition. In the present work a quite simple combustion model, based on the eddy break-up concept, originally proposed by Spalding(1977) and modified by Magnussen(1978) is used for diffusion and premix combustion. For this model, three transport equations are solved for: a passive mixing rate scalar which is equal to 1 in pure fuel regions and to zero in pure air regions and mass fraction of fuel and oxidant in flow.

Using the above mentioned combustion and turbulence model, a three-dimensional numerical code to solve the turbulent combustion in gas turbine combustor is developed on the basis of Semi-Implicit Method for Pressure Linked Equations (SIMPLE) scheme of Patankar(1980). The applicability of this procedure as a computational tool to the gas turbine design process is verified by carrying out validation study. In the validation studies of turbulence and combustion models used in the present method, several test cases available in the open literature are selected as containing, in whole or in part, features encountered in gas turbine combustors. As the test cases are considered the confined sudden expansion flow, the swirling diffusion and premix combustion, and the industrial combustor. The findings of this study are presented in the results and discussion section.

2. GOVERNING EQUATIONS

In this section, attention is focused on the formulation of the equations governing the conservation of mass, momentum, energy and chemical species for three-dimensional variable density, variable viscosity flows. Based on the conventional time averaging, the equations of motion in cylindrical coordinate system best suited to the geometry of most gas turbine combustors can be written as follows;

Continuity Equation

$$\frac{1}{r}\frac{\partial}{\partial r}(r\rho v)+\frac{1}{r}\frac{\partial}{\partial \theta}(\rho w)+\frac{\partial}{\partial x}(\rho u)=0 \qquad (1)$$

r-Momentum Equation

$$\rho\left(v\frac{\partial v}{\partial r}+\frac{w}{r}\frac{\partial v}{\partial \theta}+u\frac{\partial v}{\partial x}-\frac{w^2}{r}\right)=-\frac{\partial p}{\partial r}+\frac{1}{r}\frac{\partial}{\partial r}\left(2r\mu\frac{\partial v}{\partial r}\right)$$
$$+\frac{1}{r}\frac{\partial}{\partial \theta}\left\{\mu\left(r\frac{\partial}{\partial r}\left(\frac{w}{r}\right)+\frac{1}{r}\frac{\partial v}{\partial \theta}\right)\right\}$$
$$-2\frac{\mu}{r}\left(\frac{1}{r}\frac{\partial w}{\partial \theta}+\frac{v}{r}\right)+\frac{\partial}{\partial x}\left\{\mu\left(\frac{\partial u}{\partial r}+\frac{\partial v}{\partial x}\right)\right\}+S_x \qquad (2)$$

θ-Momentum Equation

$$\rho\left(v\frac{\partial w}{\partial r}+\frac{w}{r}\frac{\partial w}{\partial \theta}+\mu\frac{\partial w}{\partial x}+\frac{vw}{r}\right)=-\frac{1}{r}\frac{\partial p}{\partial \theta}$$
$$+\frac{1}{r}\frac{\partial}{\partial r}\left\{r\mu\left(r\frac{\partial(w/r)}{\partial r}+\frac{1}{r}\frac{\partial v}{\partial \theta}\right)\right\}+\frac{\mu}{r}\left\{r\frac{\partial}{\partial r}\left(\frac{w}{r}\right)+\frac{1}{r}\frac{\partial v}{\partial \theta}\right\}$$
$$+\frac{1}{r}\frac{\partial}{\partial \theta}\left\{\mu\left(\frac{2}{r}\frac{\partial w}{\partial \theta}+\frac{2v}{r}\right)\right\}+\frac{\partial}{\partial x}\left\{\mu\left(\frac{\partial w}{\partial x}+\frac{1}{r}\frac{\partial u}{\partial \theta}\right)\right\}+S_y \qquad (3)$$

x-Momentum Equation

$$\rho\left(v\frac{\partial u}{\partial r}+\frac{w}{r}\frac{\partial u}{\partial \theta}+u\frac{\partial u}{\partial x}\right)=-\frac{\partial p}{\partial x}$$

$$+\frac{1}{r}\frac{\partial}{\partial r}\left\{r\mu\left(\frac{\partial u}{\partial r}+\frac{\partial v}{\partial x}\right)\right\}+\frac{1}{r}\frac{\partial}{\partial \theta}\left\{\mu\left(\frac{1}{r}\frac{\partial u}{\partial \theta}+\frac{\partial w}{\partial x}\right)\right\} \quad (4)$$

$$+\frac{\partial}{\partial x}\left(2\mu\frac{\partial u}{\partial x}\right)+S_z$$

In the above equations u, v and w are the component velocities in the directions x, r and θ, respectively; p is the pressure; ρ and μ are, respectively, the density and viscosity of the fluid. S_x, S_y and S_z stand for the momentum source terms. In the present case of turbulent flow, μ and p stand for laminar viscosity and static pressure augmented by their turbulent counterparts. The evaluation of the turbulent viscosity involves the representation of turbulence by a suitably designed turbulence model, which will be discussed next.

2.1 Turbulence Model

Since in the gas turbine combustor proper mixing of fuel and oxidant is achieved by introducing the oxidant into the combustor chamber through the inlet after a swirl motion being added, it is very important to consider the effect of swirl in the modeling of turbulence phenomena. Characteristics of local turbulence in the present work is accomplished by a k-ε turbulent model improved to take into account the effect of swirling turbulent flows. Since it is well known that the k-ε model in its standard form is not adequate for taking into account the secondary straining effect of swirl. According to Bradshaw (1969) the secondary straining increases or decreases the turbulent length scale in the flow field depending on the stability of the straining field. In the standard k-ε model, the eddy viscosity μ_t is given by a function of turbulent kinetic energy k and its dissipation rate ε as;

$$\mu_t=\rho c_\mu\frac{k^2}{\varepsilon} \quad (5)$$

Where, the model constant c_μ has a constant value of 0.09. The standard transport equations for k and ε are as follows;

$$\rho\left(v\frac{\partial k}{\partial r}+\frac{w}{r}\frac{\partial k}{\partial \theta}+u\frac{\partial k}{\partial x}\right)$$

$$=\frac{1}{r}\frac{\partial}{\partial r}\left(r\frac{\mu_t}{\sigma_k}\frac{\partial k}{\partial r}\right)+\frac{1}{r}\frac{\partial}{\partial \theta}\left(\frac{\mu_t}{\sigma_k}\frac{1}{r}\frac{\partial k}{\partial \theta}\right)+\frac{\partial}{\partial x}\left(\frac{\mu_t}{\sigma_k}\frac{\partial k}{\partial x}\right)$$

$$+G_k-\rho\varepsilon \quad (6)$$

$$\rho\left(v\frac{\partial \varepsilon}{\partial r}+\frac{w}{r}\frac{\partial \varepsilon}{\partial \theta}+u\frac{\partial \varepsilon}{\partial x}\right)=\frac{1}{r}\frac{\partial}{\partial r}\left(r\frac{\mu_t}{\sigma_\varepsilon}\frac{\partial \varepsilon}{\partial r}\right)$$

$$+\frac{1}{r}\frac{\partial}{\partial \theta}\left(\frac{\mu_t}{\sigma_\varepsilon}\frac{1}{r}\frac{\partial \varepsilon}{\partial \theta}\right)+\frac{\partial}{\partial x}\left(\frac{\mu_t}{\sigma_\varepsilon}\frac{\partial \varepsilon}{\partial x}\right)+\left(c_{\varepsilon 1}G_k-c_{\varepsilon 2}\rho\varepsilon\right)\frac{\varepsilon}{k} \quad (7)$$

Where, G_k, the production rate term of k is written as;

$$G_k=\mu_t\left(2\left(\left(\frac{\partial u}{\partial x}\right)^2+\left(\frac{\partial v}{\partial r}\right)^2+\left(\frac{1}{r}\frac{\partial w}{\partial \theta}+\frac{v}{r}\right)^2\right)\right.$$

$$\left.+\left(\frac{\partial w}{\partial x}+\frac{1}{r}\frac{\partial u}{\partial \theta}\right)^2\right)+\left(\frac{\partial u}{\partial r}+\frac{\partial v}{\partial x}\right)^2+\left(\frac{\partial w}{\partial r}+\frac{1}{r}\frac{\partial v}{\partial \theta}-\frac{w}{r}\right)^2 \quad (8)$$

and the model constants are σ_k=1, σ_ε=1.3 , $c_{\varepsilon 1}$=1.44, and $c_{\varepsilon 2}$=1.92.

In order to take into account the secondary straining effect of swirl, the approach first proposed by Kim and Chung (1987) is used. Based on their approach, an improved k-ε model for swirling flows is developed by formally operating on the algebraic Reynolds stress model proposed by Rodi (1976) to modify eddy viscosity. This can be done by writing Rodi's model in terms of alternate coefficients as

$$\frac{\overline{u_i u_j}}{k}=\phi_1\frac{(G_k)_{ij}}{\varepsilon}+\phi_2\delta_{ij} \quad (9)$$

Where,

$$\phi_1=\frac{1-c_2}{(G_k/\varepsilon)+c_1-1} \quad \text{and}$$

$$\phi_2=\frac{\frac{2}{3}c_2(G_k/\varepsilon)+c_1-1}{(G_k/\varepsilon)+c_1-1} \quad (10)$$

The constants c_1 and c_2 are inertial and forced return-to-isotropy constants, respectively. δ_{ij} is Kronecker delta and $(G_k)_{ij}$ is the production tensor of the Reynolds stresses;

$$(G_k)_{ij}=-\overline{u_i'u_k'}\frac{\partial u_j}{\partial x_k}-\overline{u_j'u_k'}\frac{\partial u_i}{\partial x_k} \quad (11)$$

By assuming weakly swirling flow, it can be shown that the dominant turbulent shear stress components can be expressed as

$$-\overline{u'v'}=\nu_t\frac{\partial u}{\partial r} \quad (12a)$$

$$-\overline{v'w'}=\nu_t\frac{\partial w}{\partial r} \quad (12b)$$

Where ν_t is a Richardson number-dependent modified eddy viscosity, defined as

$$\nu_t=\frac{\alpha}{1+\beta Ri}\frac{k^2}{\varepsilon} \quad (13)$$

$$\text{Where, } Ri=\frac{k^2}{\varepsilon^2}\frac{w}{r}\frac{\partial w}{\partial r},\ \alpha=\phi_1\phi_2,\ \beta=4\phi_1^2 \quad (14)$$

In order to match the variable eddy viscosity model Eq.(14) to the constant coefficient model Eq.(5) for the case of vanishing Richardson number Ri, α must be equal to c_μ (=0.09). Since the return-to-isotropy constants c_1 and c_2 have been used in the literature in the ranges $1.5\le c_1\le 1.8$ and $0.5\le c_2\le 0.8$, the new model constant β should be in the range of $0.05\le\beta\le 0.44$ under the local equilibrium assumption $G_k=\varepsilon$. In the work of Kim-Chung(1987) β=0.25 is chosen as the average value of this range. However, on the basis of Eq.(14), this set of values (α=0.09, β=0.25) corresponds to $\phi_1=0.25$ and $\phi_2=0.36$. These values of ϕ_1 and ϕ_2 do not,

however, compatible with each other. This can be shown by letting $G_k/\varepsilon=1$ in Eq.(10) and noting that

$$\phi_1 = \frac{1-c_2}{c_1} \text{ and } \phi_2 = \frac{2(1-\phi_1)}{3} \quad (15)$$

so that $3\phi_2 = 2(1-\phi_1)$ (16)

which is not satisfied when $\phi_1 = 0.25$ and $\phi_2 = 0.36$. Also, these specified values violate the constraint that $\overline{u_i' u_i'} / k = 2$. In order to include the wall effects of local strain behavior to apply the model to complicated swirling flows like combustor in the present work the following approach is used. The present approach is to substitute c_μ / ϕ_1 for ϕ_2 in Eq.(16), which yields a quadratic equation for ϕ_1. The solution of this equation can be written as

$$\phi_1 = \frac{1 \pm (1-6c_\mu)^{1/2}}{2} \quad (17)$$

From which $\phi_1 = 0.16$ (negative root) and $\phi_2 = 0.56$ when c_μ=0.09. These values for ϕ_1 and ϕ_2 satisfy the constraint $\overline{u_i' u_i'} / k = 2$ and these values are used to decide the values of α and β

2.2 Combustion Process.

In addition to the conservation equations , other equations are needed to determine the distribution of "combustion-borne" variables. The necessity for this is apparent when the density is specified in the following general manner:

$$\rho = \rho(p, T, m_j's) \quad (18)$$

Where T is the temperature of the fluid mixture and m_j's are the mass fractions of the component species of the mixture. In this context, the additional equations required for the prediction of gaseous combustion are the enthalpy equation, concentration equations, expressions relating the auxiliary parameters to the dependent variables together with models for combustion.

Enthalpy Equation

The stagnation enthalpy h, is defined as :

$$h = C_p T + m_{fu} H_{fu} + \frac{u^2 + v^2 + w^2}{2} \quad (19)$$

Where, H_{fu} is the heat of combustion, m_{fu} is the mass fraction of unburned fuel in the mixture and C_p is the specific heat of the mixture at constant pressure.

Employing the first law of thermodynamics and neglecting the contribution of the kinetic energy of mean motion yields the following expression for h:

$$\rho\left(v\frac{\partial h}{\partial r} + \frac{w}{r}\frac{\partial h}{\partial \theta} + u\frac{\partial h}{\partial x}\right) = \frac{1}{r}\frac{\partial}{\partial r}\left(\frac{r\mu_t}{\sigma_{t,h}}\frac{\partial h}{\partial r}\right) + \frac{1}{r}\frac{\partial}{\partial \theta}\left(\frac{\mu_t}{\sigma_{t,h}}\frac{1}{r}\frac{\partial h}{\partial \theta}\right) + \frac{\partial}{\partial x}\left(\frac{\mu_t}{\sigma_{t,h}}\frac{\partial h}{\partial x}\right) + S_h \quad (20)$$

where, S_h may include the radiation sources. Radiation modeling is not considered here. The turbulent Prandtl number for enthalpy $\sigma_{t,h}$ is 0.9. The effect of turbulent fluctuations are not considered in this investigation.

Species Concentration Equation

$$\rho\left(v\frac{\partial m_j}{\partial r} + \frac{w}{r}\frac{\partial m_j}{\partial \theta} + u\frac{\partial m_j}{\partial x}\right) = \frac{1}{r}\frac{\partial}{\partial r}\left(r\frac{\mu_t}{\sigma_{t,j}}\frac{\partial m_j}{\partial r}\right) + \frac{1}{r}\frac{\partial}{\partial \theta}\left(\frac{\mu_t}{\sigma_{t,j}}\frac{1}{r}\frac{\partial m_j}{\partial \theta}\right) + \frac{\partial}{\partial x}\left(\frac{\mu_t}{\sigma_{t,j}}\frac{\partial m_j}{\partial x}\right) + R_j \quad (21)$$

where, m_j is the mass fraction of species j in the mixture and R_j is the mass rate of creation or depletion of species j by chemical reactions. This chemical reaction rate is generally a function of temperature and m_j. In the present work three transport equations are solved: a passive mixing rate scalar, which is equal to 1 in pure fuel regions and to 0 in pure air regions, mass fraction of fuel and mass fraction of oxidant in the flow.

Combustion Model

For single-phase combustion the reaction process is influenced by the mixing rate of reactants and chemical kinetics. In cases with no initial mixing of the fuel and oxidant, that is, the diffusion flame, the mixing rate governs the reaction process, i.e., thermodynamic equilibrium exists throughout. The implication of this is that the reaction will go to completion instantaneously once the mixing of fuel and oxidant has been achieved on a molecular level. Whereas, premixed flames are generally identified with chemical kinetics playing as significant a role as the mixing process. The reaction rate term of the mass fraction of fuel m_{fu} equation can be expressed in the absence of turbulence via the familiar, bi-molecular Arrhenius relation:

$$R_{fu,1} = Z\rho^2 m_{fu} m_{ox} e^{(-E/RT)} \quad (22)$$

where $R_{fu,1}$ is rate obtained by chemical kinetics alone, Z is Pre-exponential coefficient and E is Activation energy.

In the present work, the influence of turbulence on reaction rate is taken into account by the combustion model proposed by Magnussen (1978). This model is based on the eddy break-up concept of Spalding (1972) and is modified to be applicable to diffusion, partially premixed, and premixed flames. The eddy break-up model assumes that the local reaction rate is proportional to the rate of dissipation of turbulent eddies. It is assumed that the eddy will burn around its edges only where the gradients in specie and temperature are high, the argument for this assumption being that the chemical reaction rate is much faster than the turbulent mixing rate. So the time it will take to burn completely is the time it will take to dissipate by the cascade process. The time required by an eddy to dissipate can be related to the time scale of turbulence, ε/k. Therefore, proper specification of turbulence intensity and the length scale of turbulence, based on the measured values, at the boundary is very important.

It is possible that in diffusion flames, a fuel containing eddy may dissipate hydrodynamically without burning because enough oxygen is not available around it. It is also possible, in premixed flames for example, that even if enough oxygen is available the mixture may not

burn because it is not hot enough. Hence, the expression for the reaction rate is formulated to take into account the above possibilities.

$$R_{fu,2} = \rho\left(\frac{\varepsilon}{k}\right) \times \min\left(A_1 m_{fu}, A_1 \cdot \frac{m_{ox}}{R}, A_2 \cdot \frac{m_{PR}}{(1+R)}\right) \quad (23)$$

Where, R is the stoichiometric ratio of oxidant and fuel by mass, m_{PR} is mass fraction of product, and A1 and A2 are constants having values of 4.0 and 2.0, respectively.

2.3 Numerical Algorithm

All the elliptic partial differential equations presented in the previous sections were written in a common form to be solved by the well-established Semi-Implicit Method for Pressure Linked Equations (SIMPLE) scheme of Patankar (1980), the detail description of this scheme is available in their report. Temperature is calculated in an iterative manner from the composition and enthalpy values using temperature versus enthalpy tables for the individual specie. Density is then calculated from the equation of state.

$$\rho = \frac{p}{R_m T\left(\frac{m_{ox}}{Mw_{ox}} + \frac{m_{fu}}{Mw_{fu}} + \frac{m_{PR}}{Mw_{PR}}\right)} \quad (24)$$

2.4 Boundary Conditions

In the calculation, specification of correct inlet length scale is very necessary due to strong dependency of the reaction rate on it's specification. An incorrect specification results in an incorrect density field. Since, density is strongly coupled to the flow field, an incorrect density changes the flow field completely. This incorrect density, especially if it is lower than the actual density, can not be corrected in the downstream region as the length scale is modified by the internal flow field. Hence, the flow field with combustion is not able to recover from an incorrect specification of the length scale.

Therefore, experimentally measured boundary values regarding velocity and turbulent quantities were used whenever possible. For those cases where boundary conditions were not fully supplied in the reference paper, an 'educated guess' was made.

3. Results and Discussion

Since the main aim of the present work is to check the validity of the performance of the two equation k-ε turbulence model modified for swirling flows and combustion model used in the flow solver, several cases were selected as containing, in whole or in part, features encountered in gas turbine combustors. Experimental data available in the open literature were used for this purpose. The test case order is one of increasing complexity as follows; (a) constant density single entry sudden expansions with a range of diameter and velocity ratios. (b) swirling premixed flame in sudden expansion. (c) Can type combustor with swirling flame having different swirl number. (d) A practical dry low Nox combustor for 1300°C class gas turbine.

Case (a): Confined Sudden Expansion Flow

Experimental data of Chaturvedi(1963) and Lipstein(1961) were used for this purpose. Chaturvedi (1963) measured the mean velocity, pressure and turbulence intensity in a sudden expansion of diameter ratio d_o/d_i of 2 (r_i =5.3975 cm and r_o =10.795 cm) for inlet flow velocity of 30.48 m/s. Initial value of turbulence kinetic energy k was not provided by the experimentor and was guessed. A total of 51X21X181 grid points in the r-, θ - and x-directions are used for the computation. A 90 degree sector model is used, assuming periodicity in angular direction. In Fig.1 is compared the measured and predicted streamlines. This figure shows that the predicted flow is expanding slightly faster than the measured one. The measured recirculation zone is well predicted. Only a slight under-prediction of the reattachment point can be seen.

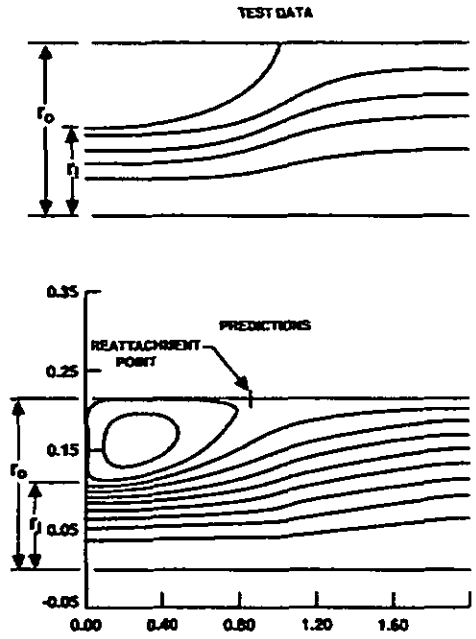

Fig. 1 Comparison of Predicted and Measured Streamlines

Figures 2-4 give the measured and predicted profiles of mean velocity u, turbulence intensity $\sqrt{u'^2}/u_o$, and pressure p, respectively at downstream distances of x/r_0 equal to 1.0, 3.0 and 8.0. The turbulence intensity is obtained from the calculated turbulence kinetic energy based on the assumption of $\sqrt{u'^2} = \sqrt{(2/3)k}$.

It can be observed from Fig.2 that the mean velocity is predicted extremely well for all the three axial locations including the

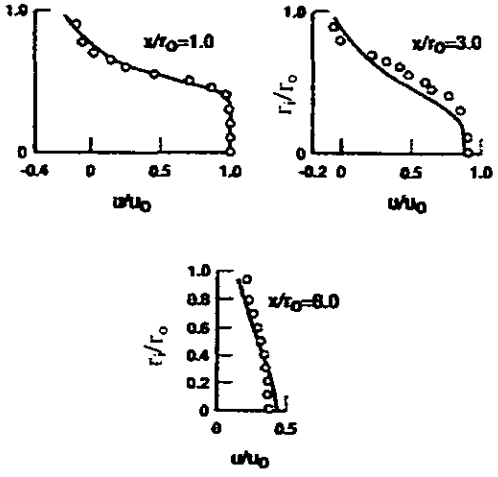

Fig.2 Radial Profiles of Mean Axial Velocity

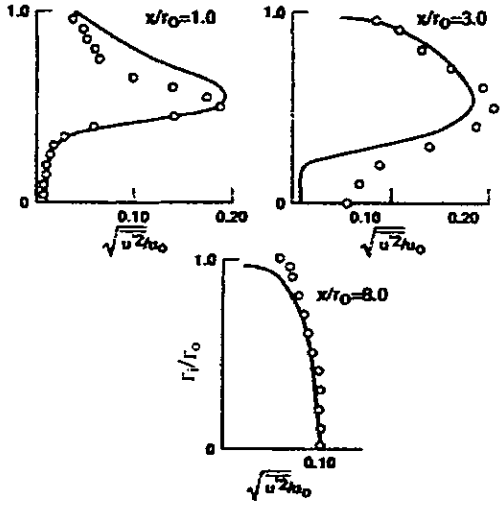

Fig.3 Radial Profiles of Mean Axial Velocity

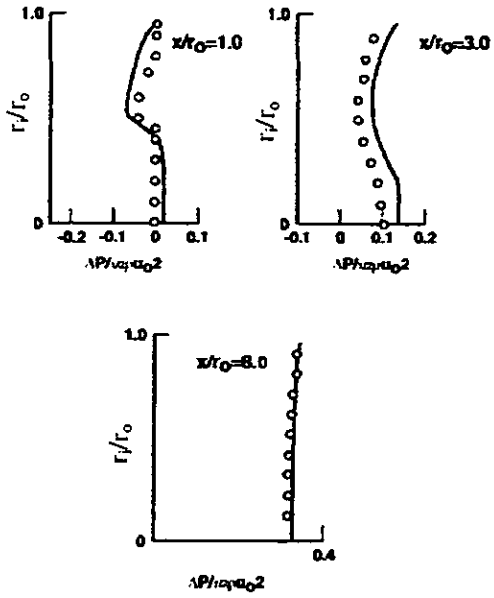

Fig.4 Radial Profiles of Static Pressure

location inside the recirculation region. Outside the recirculation zone the agreement between measured and predicted turbulence intensity is very satisfactory, as Fig.3 indicates. Inside the recirculation region also the measured turbulence intensity profile is predicted quite reasonably. Considering the guess of inlet turbulence condition, this agreement is expected to be satisfactory. As Fig.4 shows, the measured pressure profiles are quite well-predicted.

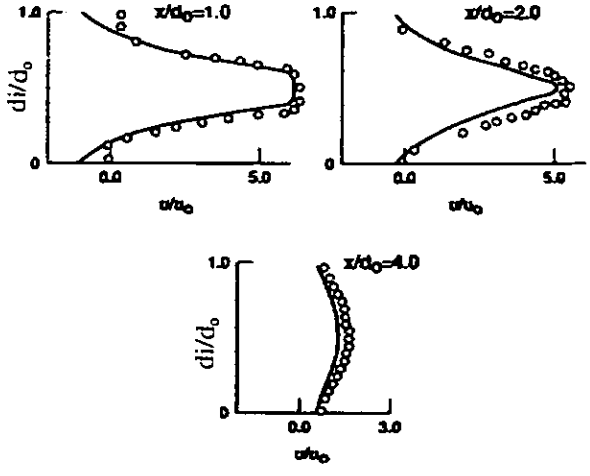

Fig.5 Mean Axial Velocity Profiles (D_j/D_o=2.5)

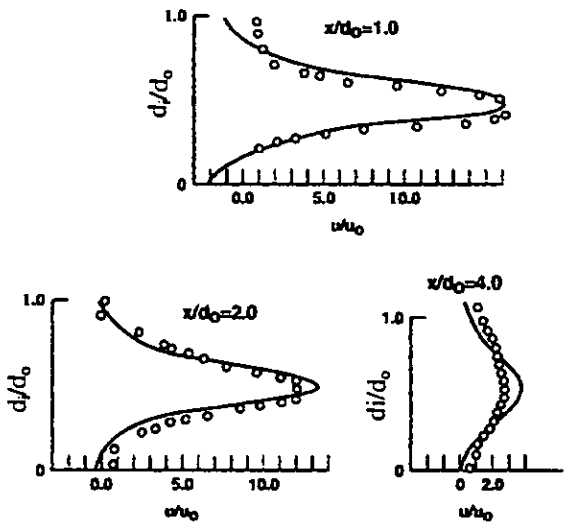

Fig.6 Mean Axial Velocity Profiles (D_i/D_o=4.0)

Figures 5-6 give the predicted and measured profiles of axial velocity (Lipstein (1961)) for diameter ratios of 2.5 and 4.0 respectively. A good agreement between the measured and predicted values is observed. The results presented here showed that the present method predicted the experimental data quite satisfactorily in sudden expansion flow cases for all the diameter ratios considered. Diameter ratios up to 4 is considered, because for the gas turbine combustor the ratios up to 3 are reasonably typical.

Case (b): Confined Premixed Flame With Swirl

One of the experiments of Beltagui and Maccallum (1975) is used for this case. They measured axial velocity, tangential velocity, static pressure and mean temperature profiles in premixed flames with various swirl angles. In the present work, predictions have been made of flames with a 30° swirler only. This particular case was selected because it had significant swirl, but the swirl angle was less than critical. In their experiments, vane swirlers with hub diameter of 10.0 mm and outer diameter of 93.0 mm were used. A swirling pre-mixed flow of city gas (mainly propane C_3H_8) and air with a fuel-air ratio of 0.105 was introduced through the swirler into the combustor of 225 mm inner diameter and 900 mm in length. The axial velocity at the inlet was 75m/s. In order to specify the dissipation rate of turbulence, the initial length scale of turbulence is calculated on the basis of spacing between swirler vanes. Thus, with this swirler design, a length scale which varied from the center of the swirler to its tip resulted. In the present computation, 56X21X191 grid points are used in the r-, θ- and x-directions, respectively. A 90 degree sector model is used, assuming periodicity in angular direction.

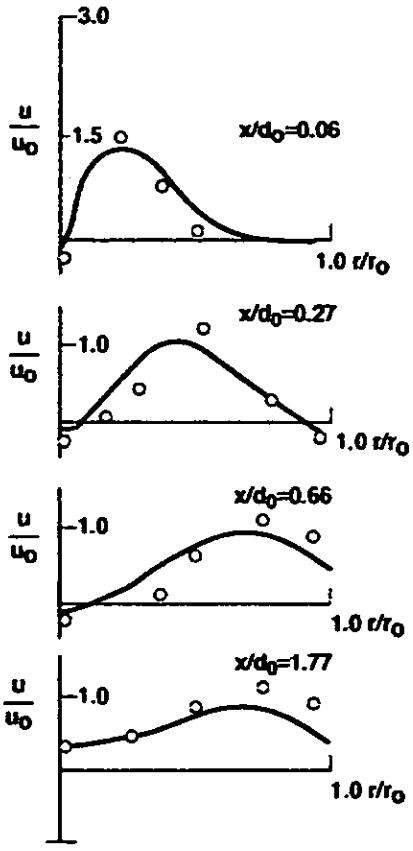

Fig.7 Mean Axial Velocity Profiles (Reacting Flow, swirl=30°)

In Fig.7 are plotted the measured and predicted axial velocity profiles at the downstream distances of x/d_0 equal to 0.06, 0.27, 0.66 and 1.77. It can be observed from this figure that the mean axial velocity are predicted quite satisfactorily, including the strength and extent of the recirculation region. For example, at x/do of 0.66, experimentally observed large but weak central recirculation with a slow velocity recovery from the centerline is predicted quite reasonably. Only the predicted central recirculation zone is slightly smaller. Further downstream at x/do of 1.77 where a central recirculation is not present, the measured values are very well predicted. . In Fig.8 and 9, measured tangential velocity and static pressure profiles are compared with the predictions. It can be seen that the comparison is again quite good.

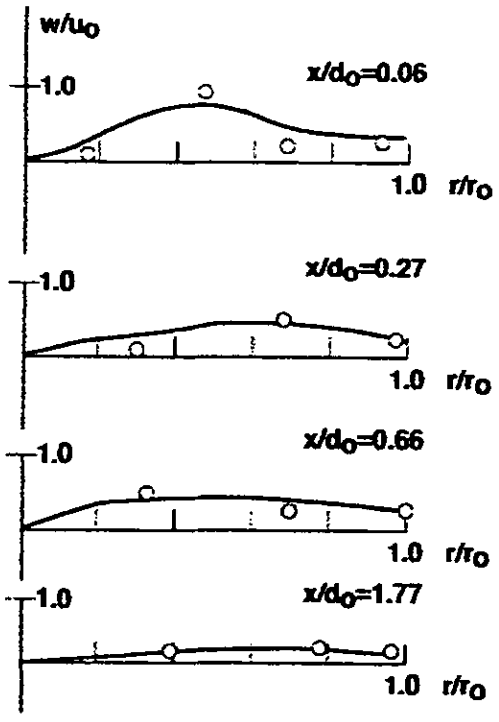

Fig.8 Tangential Velocity Profiles (Reacting Flows, Swirl=30^o)

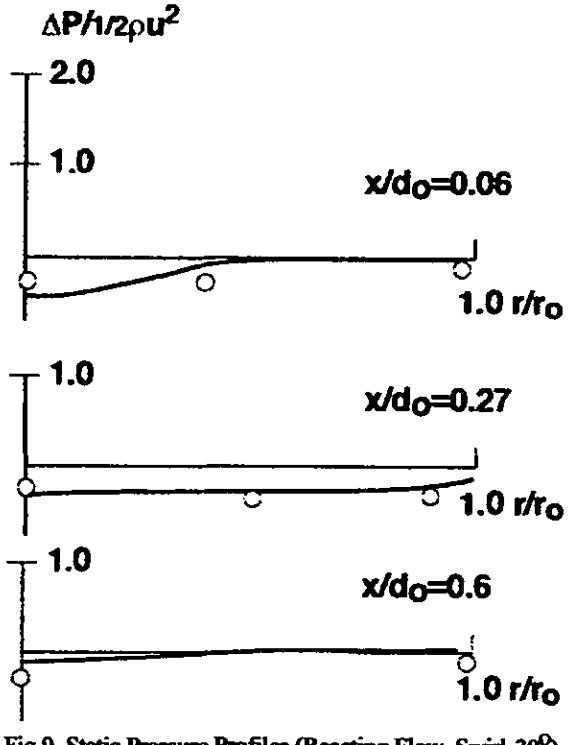

Fig.9 Static Pressure Profiles (Reacting Flow, Swirl-30^o)

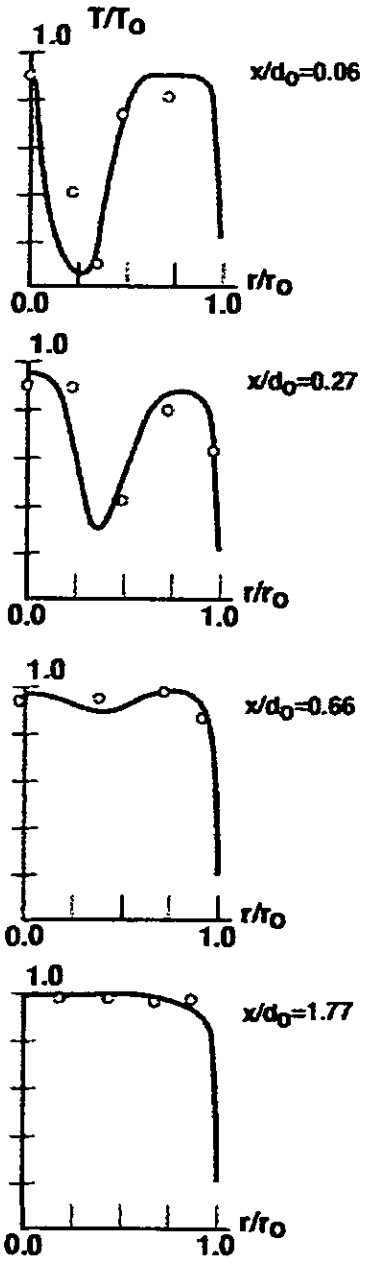

Fig.10 Mean Temperature Profiles (Reacting Flow, Swirl=30^o)

In Fig.10 is presented the comparison of measured and predicted mean temperature profiles. The temperature T_0 in this figure is 1700 K. It can be seen that the mean temperatures are predicted quite satisfactorily. In the initial region, there is a high temperature on the swirler axis followed by a temperature trough and again, high temperature near walls. The high temperatures in the center and near the wall are caused by the central and peripheral recirculation zones being established in the flow field; the central recirculation close to the swirler is assisted by the physical presence of the small swirler hub. The width of the high temperature region in the center is slightly under-predicted at x/d_0 of 0.06 and 0.27. This under-prediction

probably results from the under-prediction of the central recirculation zone. However, in such regions of high gradients, the effects of positional errors in the experiment could be significant. The temperature trough in the profiles at x/d_0 of 0.06 and 0.27 is predicted well.

Case (c): Can Type Cambastor

The combustor used in the experiment of Nakamura et al. (1991), shown in Fig.11, was a can-type one with a quartz glass liner of 100 mm inner diameter and 350 mm in length to visualize the flame and to make a LDV measurement. The combustion air was introduced into the combustion chamber through an annular air inlet of 21 mm inner diameter and 42 mm outer diameter after a swirl motion being added. Pure propane (C_3H_8) for industrial use was injected through a multihole injection nozzle. The fuel to air mass flow ratio was 0.064. They performed experiments for swirl number of 0.7, 1.0 and 1.5 by keeping the flow rate same, to study the effects of swirl strength. The mean velocity at the combustor inlet was specified as 3.15 m/s from the experiment. The turbulence intensity level is guessed. The length scale is specified as a function of distance of swirler inlet. A total of 51X21X121 grid points are used in the r-, θ- and x-directions, respectively. A 90 degree sector model is used, assuming periodicity in angular direction.

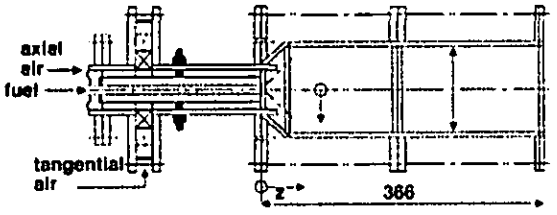

Fig.11 Schematic View of Can Type Combustor

In fig.12 and 13 are presented the measured and predicted stream line contours for swirl number of 0.7, 1.0 and 1.5. In fig.14 and 15 are presented the measured and predicted isothermal line contours. In the experiments, the swirl number was varied by keeping the mass flow rate of fuel and air constant. The stream lines represent the equi-mass flow lines of combustion gas in the combustion region, which are calculated on the basis of the following equations;

$$\psi = \int_0^r \rho u r dr \text{ and } \psi_0 = \int_0^R \rho u r dr \qquad (25)$$

where, r is radial distance in (m), R is combustor liner radius(m), ρ is density of combustion gas (kg/m^3) and u is axial velocity component (m/s).

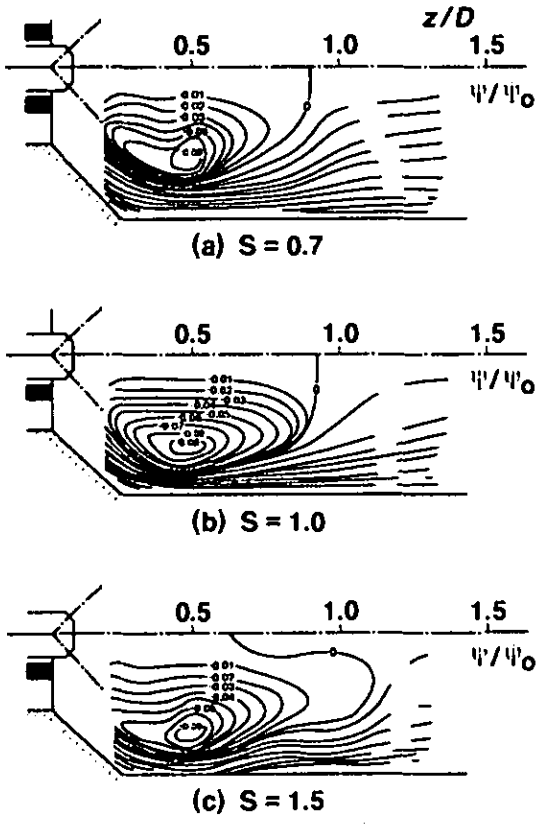

Fig.12 Measured Stream Line Contour

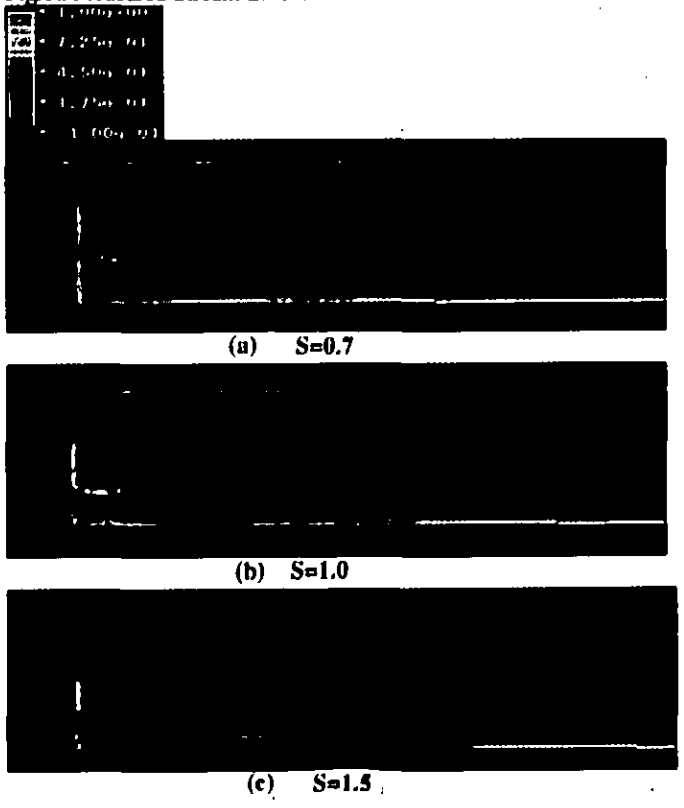

Fig.13 Predicted Stream Line Contour

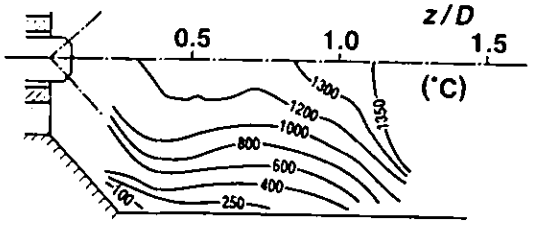

(a) S = 0.7

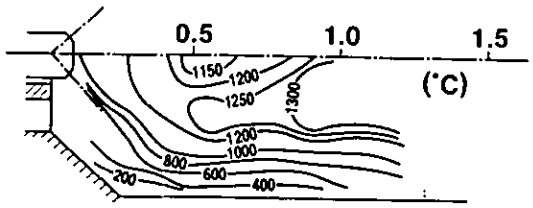

(b) S = 1.0

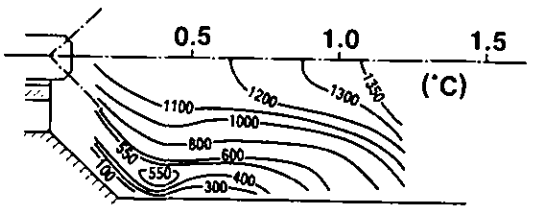

(c) S = 1.5

Fig.14 Measured Temperature Contour

(a) S=0.7

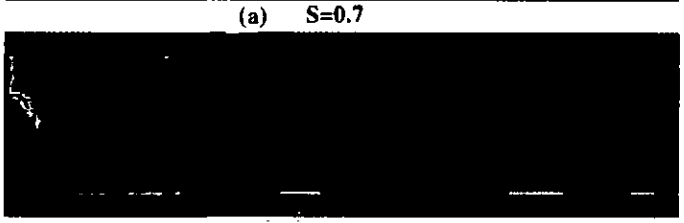

(b) S=1.0

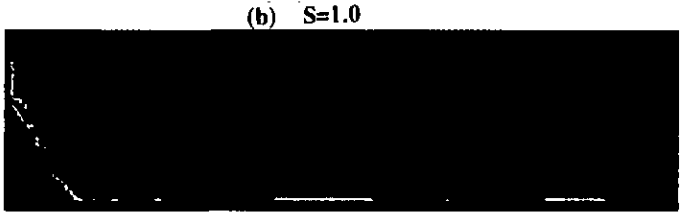

(c) S=1.5

Fig.15 Predicted Temperature Contour

The measured stream line contours presented in Fig.12 show that for all the swirl numbers considered, a recirculation zone is developed near the fuel injector, and the flame is stabilized by the zone while the vortex center and the recirculation boundary shifts to the liner wall side due to the increase of angular momentum of combustion gas flow with the swirl strength. This recirculation zone extends with the increase of swirl number. Experimentally observed phenomena are predicted quite satisfactorily as can be seen from Fig.13. Only the extension of the recirculation zone is slightly under-predicted. Considering the guess of inlet turbulence condition, this agreement is thought to be good.

It can be observed from the measured and predicted isothermal lines presented in Fig.14 and 15 that since a recirculation zone develops in this range of swirl number, as indicated in Fig.12 and 13, there are no large difference between them and the region near the injection nozzle presents a high temperature. When the swirl number is increased, the temperature profile indicates that the flame gets spread out to the outside. These experimentally observed phenomena are predicted quite reasonably. Also, the maximum temperature level of combustor is predicted within an error level of 5 to 7%.

Case (d): Low-Nox Praetical Combustor

In Fig.16 is shown a schematic view of a 1300°C class dry low NOx combustor. The fuel and oxidant were introduced into the combustor through the inlet and through the combustor outer wall. At the inlet a small portion of the total fuel was introduced into the combustor through a fuel injector located near the centerline and the air for combustion was supplied through the swirler. Also introduced through the inlet was pre-mixed fuel and air as the pilot fuel to the combustor. Pre-mixed air and rest of the total fuel served as the main fuel were introduced into the combustor through three axial locations of combustor outer wall at 45 degree angular spacing. The velocity of the premixed flow at the inlet was about 65 m/s. The velocity of the inlet swirler air and of the premixed flow from the outer wall were 45m/s and 95m/s, respectively. A total of 56X42X168 grid points were used in r- , θ- and x-directions, respectively. Computations were carried out for 90 degree sector model, assuming the flow in angular direction is periodic. The main purpose of this computation is to have some understanding of the complex flow and temperature field in the combutor, which is very much necessary for the design and development process. Because, it

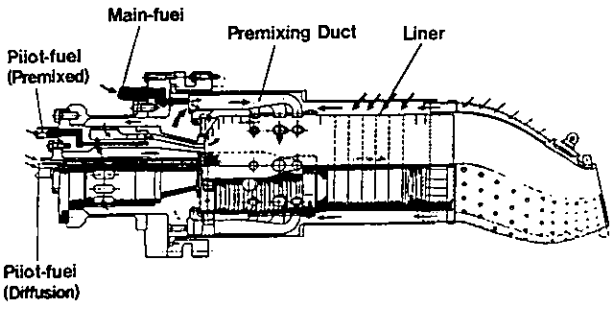

Fig.16 1300OC Class Dry Low Nox Combustor

is extremely difficult to obtain reliable and extensive measurements in practical combustor at its design operating point.

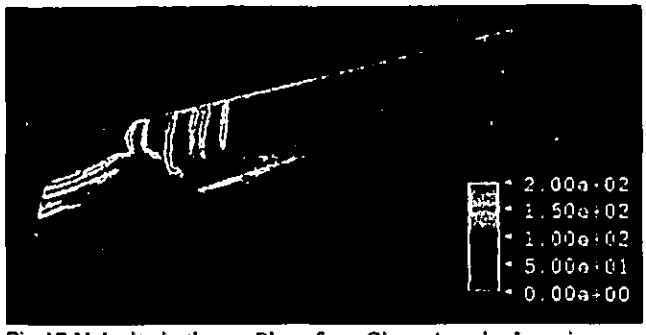

Fig.17 Velocity in the r-x Plane for a Given Angular Location

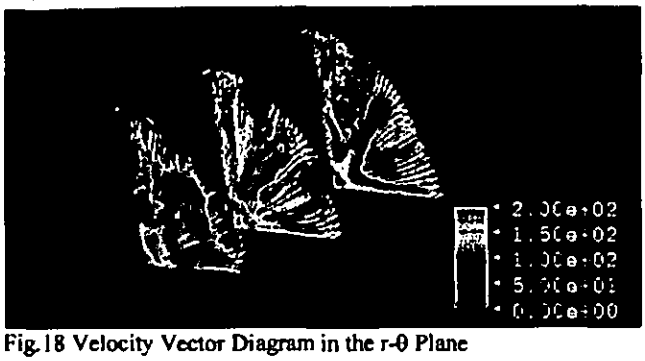

Fig.18 Velocity Vector Diagram in the r-θ Plane

In Fig.17 is presented the velocity contour in the r-x plane at certain angular location. This figure shows that the interaction of the flow from the inlet (swirler and premixed flows) with the jet flow from the outer wall made the flow very complicated downstream the jet and a very complex flow mixing occur in the region of interaction. At the downstream behind the jet a large recirculation zone is developed with reattachment at further downstream. In Fig.18 is presented the velocity vector diagram in r-θ plane at three different x-locations. The upstream vector diagram of this figure indicates that a pair of vortices is developed near the outer wall due to the interaction of the swirling flow coming from the inlet with the jets from outer wall. The central vector diagram shows the flow field of the jets and its surroundings. The downstream vector diagram shows a pair of flow vortices developed by the interaction of main flow with the jet.

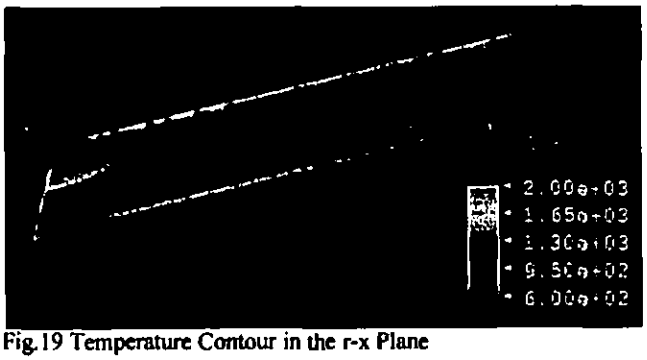

Fig.19 Temperature Contour in the r-x Plane

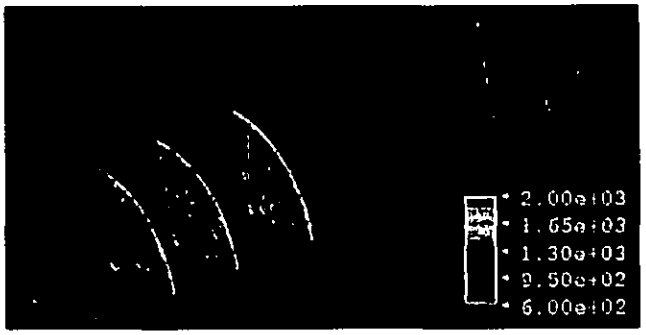

Fig.20 Temperature Contour in the r-θ Plane

In Fig.19 and 20 are presented the predicted temperature contour in the combustor. Figure 19 shows the temperature contour in the r-x plane at certain angular location. It can be observed here that in the region where the inlet flame mixed with the premixed flame from combustor outer wall the temperature is high. At the downstream behind the jet because of the development of recirculation zone, as indicated in Fig.17, the flame gets spread out to the outer wall. Figure 20 show the temperature contour in r-θ plane at three different x locations (same as Fig.18). This figure indicates that in the upstream region the temperature in the angular direction is quite uniform, except near the outer wall where due to the interaction between the inlet flame and the jet there exist a temperature trough and a high temperature region in the angular direction. The central diagram of this figure shows the temperature profile of the jet. The downstream contour diagram indicates two high temperature pockets with a temperature trough in between. The measured average exit temperature in this case is predicted within an error level of about 15%.

4. CONCLUSIONS

The main purpose of the present work is to evaluate the performance of the turbulence and combustion models used in the development of an efficient computational tool for the gas turbine combustor design. Since in the gas turbine combustor mixing of fuel and oxidant is achieved by introducing the oxidant into the combustion chamber after a swirl motion being added. A two-equations k-ε turbulence model is modified for swirling turbulent flows by operating on the algebraic Reynolds stress model. This approach is considerably cost-effective compared with the Reynolds stress model due to the computational simplicity of the k-ε model. In the evaluation study experiments have been selected from those available in the literature. This study led to the following findings;

In the case of sudden expansion flows with different diameter ratios, the profiles of various quantities are predicted very well. In the case of swirling flows, a recirculation zone is developed near the center of the channel. The size and the strength of the recirculation zone increase due to the increase of angular momentum of flow with the swirl strength. The measured temperature profiles indicate that the flame spreads out to the outside with the increase of swirl number. The k-ε model improved for swirling flows predicted the profiles of various quantities quite satisfactorily. The size and strength of the

recirculation zone are predicted reasonably.

The results of computation for practical dry low-Nox combustor gave a good understanding of the complicated flow behavior and the combustion process. Nevertheless, the validation study of the present k-ε and combustion model will be continued with some more experimental data on diffusion and premixed combustion for swirling flows

REFERENCES

Beltagui, S. A. and Maccallum, N. R. L., 1975, "The Aerodynamic Modeling of Vane-Swirled Premixed Flames in Furnaces," Proceedings of first joint Aerodynamic and Heat Transfer Panel Meeting, Toulouse, France

Bradshaw, P., 1969, "The analogy between Streamline Curvature and Boyancy in Turbulent Shear Flow," Journal of Fluid Mechanics, Vol.36, pp.177-191.

Chaturvedi, M. C., 1963, "Flow Characteristics of Axisymetric Expansions," Journal of the Hydraulics Division, Proceedings of ASCE, pp.1.

Kanniche, M. and Zurbach, S., 1995, "Coherent Flame Model For Turbulent Combustion Operating with both Premixed and Non-Premixed Flames," ASME Paper No. 95-GT-168.

Kim, K. Y. and Chung, M. K., 1987, "New Eddy Viscosity Model for Computation of Swirling Turbulent Flows," AIAA Journal, Vol.25, No.7, pp.1020-1021.

Lipstein, N. J., 1961, "Low Velocity Sudden Expansion Pipe Flow," General Electric Report No. GIGL 213.

Magnussen, B. F. and Hjetager, B. H., 1978, "On Mathematical Modeling of Turbulent Combustion with Special Emphasis on Soot Formation and Combustion," The Sixteenth Symposium (International) on Combustion, The Combustion Institute, pp.719-729.

Nakamura, S., Hyodo, K. and Kawaguchi, O., 1991, "The Structure and Stabilization Mechanism of the Primary Region of a Model Gas Turbine Combustor," Proceedings of International Gas Turbine Conference, Yokohama, Japan, Yokohama-IGTC-48.

Novick, A. S., Miles, G. A. and Lilley, D. G., 1979, "Modeling Parameter Influences in Gas Turbine Combustor Design," AIAA Paper 79-354.

Patankar, S. V., 1980, "Numerical Heat Transfer and Fluid Flow," McGraw-Hill.

Rodi, W., 1976, "A New Algebraic Relation for Calculating the Reynolds Stress," ZAMM, Vol.56, pp. T219-221.

Spalding, D. B., 1977, "A General Theory of Turbulent Combustion; The Lagrangian Aspects," AIAA Paper no. 77-0141.

Speziale, C. G., 1991, "Analytical Methods for the Development of Reynolds Stress Closures in Turbulence," Annual Review of Fluid Mechanics, Vol.23, pp.107-157.

Sturgess, G. J., 1980, "Gas Turbine Combustor Liner Durability - The Hot Streak Problem," Proceedings of a Project SQUID Workshop "Gas Turbine Combustor Design Problems," Hemisphere Publishing Corporation, pp. 133-150.

Sturgess, G. J. and Syed, S. A., 1985, "Calculation of Confined Swirling Flows," AIAA Paper 85-0060.

Vanka, S. P., 1985, "Calculation of Axisymetric Turbulent Confined Diffusion Flames," AIAA Paper 85-0141.